

# Tailoring of the $\alpha$ -, $\beta$ -, and $\gamma$ -Modification in Isotactic Polypropene and Propene/Ethene Random Copolymers

Karsten Busse\* and Jörg Kressler

Martin-Luther-Universität, Fachbereich Ingenieurwissenschaften, Institut für Bioengineering,  
D-06099 Halle (Saale), Germany

Ralph-Dieter Maier

BASF AG, Abteilung Polyolefine, ZKP/T - M510, D-67056 Ludwigshafen, Germany

Jonas Scherble

Albert-Ludwigs-Universität Freiburg, Institut für Makromolekulare Chemie, Stefan-Meier-Str. 21,  
D-79104 Freiburg i.Br., Germany

Received April 25, 2000; Revised Manuscript Received September 5, 2000

**ABSTRACT:** An isotactic polypropene (i-PP) prepared with a metallocene catalyst system and two random copolymers of propene and ethene with 2.8 and 5.7 wt % ethene, respectively (PP-co-E-2.8, PP-co-E-5.7), were isothermally crystallized during simultaneous small- and wide-angle X-ray scattering (SAXS, WAXS) in synchrotron measurements. Identical measurements were carried out after adding 0.3 wt % *N,N*-dicyclohexyl-2,6-naphthalene dicarboxamide, a  $\beta$  nucleating agent ( $\beta$ -NA). All samples form the  $\gamma$ -modification to a certain extent. WAXS data show that the  $\alpha$ -modification is predominant in i-PP, PP-co-E-2.8, and PP-co-E-5.7 isothermally crystallized without  $\beta$ -NA at temperatures below 125 °C. Adding  $\beta$ -NA leads to significant amounts of the  $\beta$ -modification at all crystallization temperatures in all three samples. Thus, the three modifications can be tailored by the crystallization regime of the nucleated samples. The simultaneous occurrence of the three modifications has also implications on the SAXS data. The formation of the  $\gamma$ -modification in addition to the  $\alpha$ -modification does not lead to a one-dimensional correlation function  $K(z)$  with two distinct long periods or lamella thicknesses. In contrast, the formation of the  $\beta$ -modification results in a long period which can be distinguished from that of the other modifications after generating  $K(z)$ .

## Introduction

The different crystalline modifications of isotactic polypropene, denoted as  $\alpha$ -,  $\beta$ -, and  $\gamma$ -modification, have been a topic of research for more than 40 years. A predominant  $\alpha$ -modification can be suppressed by the occurrence of the  $\gamma$ - or  $\beta$ -modification. The  $\gamma$ -modification, unique in the field of synthetic polymers due to the nonparallel chain packing of the  $3_1$ -helices in the unit cell,<sup>1</sup> can be induced for example by the application of high pressure during the crystallization process,<sup>2,3</sup> in random copolymers of propene with 2.5–20 wt % of other 1-olefins,<sup>4–10</sup> by the crystallization in shear fields, by using very low molecular mass samples, or in isotactic polypropene samples prepared with a metallocene catalyst system, due to structural defects.<sup>11–13</sup> Quenching conditions in order to obtain the  $\beta$ -modification of isotactic polypropene were discovered by Padden and Keith<sup>14,15</sup> and by Turner-Jones et al.<sup>16</sup> Nowadays, a number of nucleating agents to achieve the formation of large amounts of the  $\beta$ -modification are available.<sup>17,18</sup> The  $\beta$ -modification is also unique in the field of crystallization of synthetic polymers due to the frustration phenomenon in polymer crystallography.<sup>19,20</sup> From a practical point of view there is some interest in the  $\beta$ -modification of isotactic polypropene caused by an improvement of mechanical properties.<sup>17</sup> Energy calculations show that the  $\beta$ -modification is less stable compared to the  $\alpha$ -modification and that the  $\gamma$ -modification is even slightly more stable than the  $\alpha$ -modifi-

cation.<sup>21–23</sup> The hexagonal  $P3_1$  space group was assigned to the  $\beta$ -modification.<sup>19,20,24</sup> The orthorhombic unit cell of the  $\gamma$ -modification is due to Meille et al.<sup>25</sup> with experimental confirmation by Lotz et al.<sup>26</sup> A general review on the crystallization behavior of isotactic polypropene is found elsewhere.<sup>27,28</sup> The assignment of the WAXS reflections was provided by Natta et al.<sup>29</sup> for the monoclinic  $\alpha$ -modification and by Brückner and Meille<sup>1</sup> for the orthorhombic  $\gamma$ -modification.

In this work it is demonstrated that the  $\beta$ -modification can be introduced additionally to the  $\alpha$ - and  $\gamma$ -modification when propene–ethene random copolymers are crystallized in the presence of a  $\beta$ -nucleating agent ( $\beta$ -NA). The ratio of the crystalline modifications can be tailored by the copolymer composition, the nucleating agent, and the temperature regime during crystallization. Three samples are used for crystallization experiments: neat isotactic polypropene prepared with a metallocene catalyst system (i-PP) and two random copolymers of propene and ethene with 2.8 and 5.7 wt % ethene, respectively (PP-co-E-2.8 and PP-co-E-5.7). *N,N*-Dicyclohexyl-2,6-naphthalene dicarboxamide is used as a  $\beta$ -NA.<sup>17</sup> The crystallization is studied by simultaneous wide- and small-angle X-ray scattering (WAXS and SAXS) experiments using synchrotron radiation.

## Experimental Section

**Materials.** The samples used for crystallization experiments were provided by BASF AG. One neat isotactic polypropene was prepared with a metallocene catalyst system (i-PP)

\* To whom correspondence should be addressed.

**Table 1. Characteristics of the Polypropylenes**

polymer	ethene content [wt %] <sup>a</sup>	ethene content [mol %] <sup>a</sup>	$\Sigma_{\text{defects}}$ [%] <sup>a,b</sup>	$M_w$ [kg/mol] <sup>c</sup>	$M_w/M_n$ <sup>c</sup>	$T_m$ [°C] <sup>d</sup>
i-PP			1.1	280	2.0	150
PP-co-E-2.8	2.8	4.0	n.d.	236	4.3	150
PP-co-E-5.7	5.7	7.1	n.d.	232	4.3	145

<sup>a</sup> <sup>13</sup>C NMR spectroscopy. <sup>b</sup> Calculated according to Fischer et al.<sup>11</sup> <sup>c</sup> GPC. <sup>d</sup> DSC, heating rate 10 °C/min; n.d. = not determined.

and two Ziegler–Natta type random copolymers of propene and ethene with 2.8 and 5.7 wt % ethene, respectively (PP-co-E-2.8 and PP-co-E-5.7). Table 1 summarizes the characteristics of the polypropylenes. All polymer samples contained 0.05 wt % Irganox 1010 and 0.05 wt % Irgafos 168 (both from Ciba Speciality Chemicals) as stabilizers. The nucleated samples contained 0.3 wt % *N,N*-dicyclohexyl-2,6-naphthalene dicarboxamide, which is known as a highly active  $\beta$ -NA without staining effects.<sup>17</sup> It was obtained from New Japan Chemicals under the trade name NJ Star NU100. The melting point of the  $\beta$ -NA is 405 °C.

**Compounding.** Introduction of the  $\beta$ -NA into the polymer was achieved by using a ZSK25 corotating twin screw extruder (Werner&Pfleiderer) at temperatures between 190 and 230 °C. Prior to extrusion, the polymer granules were coated with the  $\beta$ -NA by mixing the respective polymer and the appropriate amount of  $\beta$ -NA by using the RRMini tumble mixer (Engelmann).

**Equipment.** Differential scanning calorimetry (DSC) measurements were performed by using a Perkin-Elmer DSC7. The samples were heated from room temperature up to 220 °C applying a rate of 10 °C/min and subsequently cooled to –40 °C at the same rate. By heating the samples again to 220 °C (at 10 °C/min), the melting points were determined. The crystallization is studied by simultaneous wide- and small-angle X-ray scattering (WAXS and SAXS) experiments using synchrotron radiation at the HASYLAB synchrotron laboratories at DESY, Hamburg.<sup>30</sup> The samples are melted at 190 °C and then isothermally crystallized at various temperatures between 105 and 140 °C. The data are taken until the degree of crystallinity remains constant. The wavelength for observations was chosen equivalent to the Cu K $\alpha$  radiation at  $\lambda = 0.154$  nm. The measured SAXS intensity is corrected for background scattering, and then the one-dimensional correlation function  $K(z)$  is calculated by cosine Fourier transformation.<sup>31,32</sup>

$$K(z) = \int_0^\infty 4\pi s^2 I(s) \cos(2\pi sz) ds \quad (1)$$

where  $I$  is the scattering intensity and  $s$  is the scattering vector. From the correlation function the values for lamella thickness, long period, and crystallinity are determined.<sup>36</sup>

## Results and Discussion

One metallocene i-PP and two random copolymers of propene and ethene with ethene contents of 2.8 and 5.7 wt %, respectively, have been used for crystallization experiments. All neat samples were crystallized, or 0.3 wt %  $\beta$ -NA was added prior to crystallization experiments. All samples show in their WAXS traces a nonvanishing  $\gamma$ -(117) peak at all temperatures applied for isothermal crystallization experiments. Figure 1a depicts the WAXS traces obtained after isothermal crystallization at 105 °C. The i-PP without  $\beta$ -NA crystallizes predominantly in the  $\alpha$ -modification, and traces of the  $\gamma$ -modification can be observed. The random copolymers have a larger amount of the  $\gamma$ -modification compared to the i-PP sample. The  $\alpha$ -to- $\gamma$  ratio can be influenced by the crystallization temperature. This is

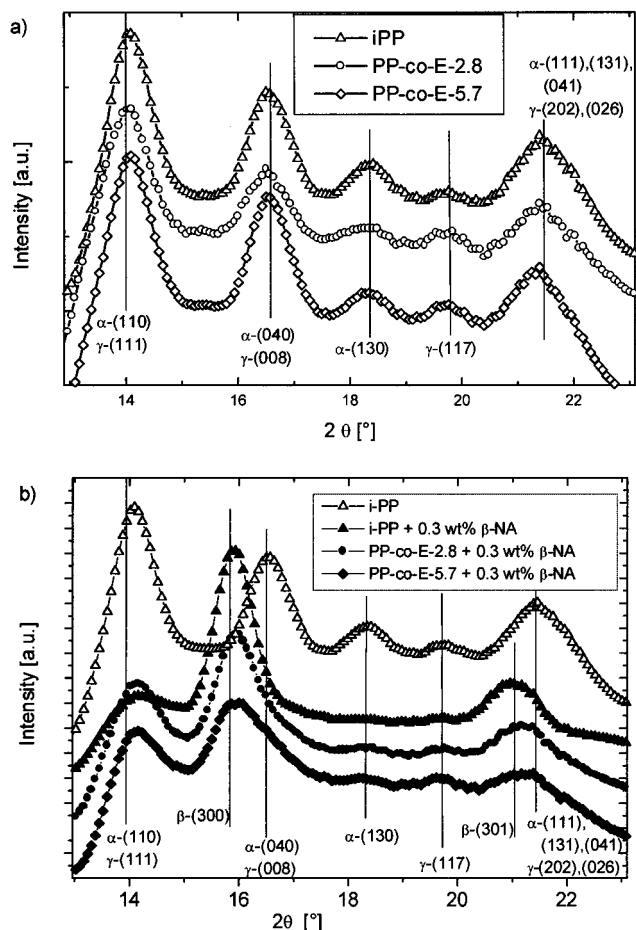


**Figure 1.** WAXS traces obtained after isothermal crystallization (a) at 105 °C for i-PP, PP-co-E-2.8, and PP-co-E-5.7 and (b) at 115 °C for i-PP and  $\beta$ -nucleated samples of i-PP, PP-co-E-2.8, and PP-co-E-5.7 with 0.3 wt %  $\beta$ -NA each.

typically observed for metallocene i-PP and discussed in detail elsewhere.<sup>11,27</sup> The  $\beta$ -modification can only be observed after the addition of certain nucleating agents. This is demonstrated in Figure 1b. The peak maximum of the reflection in the range of approximately  $15^\circ < 2\theta < 17.5^\circ$  is shifted to smaller angles for samples with  $\beta$ -NA compared to samples without  $\beta$ -NA. This is due to the fact that the chosen resolution for WAXS measurements in the high-temperature regime does not allow for separation of the  $\alpha$ -(040) and  $\gamma$ -(008) peaks at about  $2\theta = 17^\circ$ <sup>10</sup> and the  $\beta$ -(300) peak at  $2\theta = 16^\circ$ . Thus, the shift of the peak maximum in the WAXS traces of samples with  $\beta$ -NA is due to the overlap of the two reflections. The same phenomenon occurs for the peak in the range  $21^\circ < 2\theta < 23^\circ$ . Also, this peak is composed of several reflections of the different modifications. From the WAXS measurements the crystallinity  $\phi$  of the samples can be obtained to be in the range of  $\phi \sim 0.3$ –0.4 for all samples in the high-temperature regime.

Quenching the samples to room temperature after isothermal crystallization at various temperatures leads to different WAXS traces as can be seen for i-PP in Figure 2. It is most characteristic that the reflections in the ranges  $15^\circ < 2\theta < 17.5^\circ$  and  $21^\circ < 2\theta < 23^\circ$  are separated and can be assigned to the different modifications. While the crystallinity increases to  $\phi \sim 0.8$ , a decrease of the amount of  $\beta$ -modification in comparison to the  $\alpha$ - and  $\gamma$ -modification is detected after the quenching procedure when compared to the samples before quenching. This is in agreement with literature

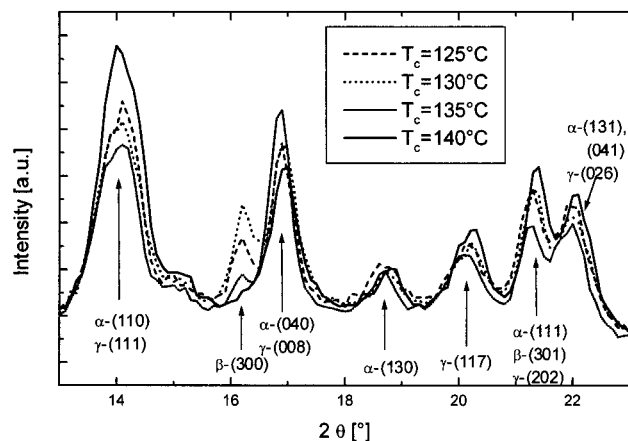


**Figure 2.** WAXS traces obtained after isothermal crystallization of i-PP with 0.3 wt %  $\beta$ -NA at different temperatures and final quenching to room temperature.

data which indicate that the  $\beta$ -modification can only be obtained at crystallization temperatures above  $100^\circ\text{C}$ .<sup>33,34</sup> From the peak heights  $h_\alpha$  of the  $\alpha$ -(130) peak and  $h_\gamma$  of the  $\gamma$ -(117) peak, the ratio  $X_{\alpha\gamma} = h_\alpha/h_\gamma$  can be evaluated directly.<sup>16</sup> But the relevant peaks for the determination of  $X_{\alpha\gamma}$  have only a small intensity at high temperatures, so the error in  $X_{\alpha\gamma}$  is large. For the samples quenched to room temperature the calculation of the ratio is more accurate. These samples have at crystallization temperatures of  $125^\circ\text{C}$  and above a ratio  $X_{\alpha\gamma}$  of about  $0.6 \pm 0.2$ . For higher crystallization temperatures, this ratio decreases very slowly. At temperatures of  $120^\circ\text{C}$  and below, there is a significant difference between the samples with and without  $\beta$ -NA. If there is any amount of  $\beta$ -modification in the sample, the ratio  $X_{\alpha\gamma}$  does not change significantly, but the samples i-PP, PP-co-E-2.8, and PP-co-E-5.7 without  $\beta$ -NA and therefore without  $\beta$ -modification contain much more  $\alpha$ -modification so the ratio  $X_{\alpha\gamma}$  increases to values between 1.3 and 2.0.

The i-PP sample crystallizes after the addition of 0.3 wt %  $\beta$ -NA nearly exclusively in the  $\beta$ -modification at moderate crystallization temperatures up to  $125^\circ\text{C}$ . Nevertheless, traces of the  $\alpha$ - and  $\gamma$ -modification can be detected. The addition of small amounts of comonomer, in this case ethene, increases generally the tendency of the formation of the  $\gamma$ -modification.<sup>13</sup> This is also indicated in Figure 1b where i-PP, PP-co-E-2.8, and PP-co-E-5.7 are crystallized at  $115^\circ\text{C}$  in the presence of 0.3 wt %  $\beta$ -NA in comparison to the neat i-PP sample at the same crystallization temperature. Basically all three modifications can be observed. In Figure 3a the time-resolved WAXS traces for i-PP at  $T_c = 115^\circ\text{C}$  in the presence of 0.3 wt %  $\beta$ -NA are shown. The formation of the  $\alpha$ - and  $\gamma$ -modification is strongly suppressed. The time-resolved WAXS traces for PP-co-E-2.8 at  $T_c = 120^\circ\text{C}$  with  $\beta$ -NA in Figure 3b show significant  $\alpha$ -(130) and  $\gamma$ -(117) peaks.

WAXS measurements are able to provide information on the crystal modification and the degree of crystallinity. Corresponding information can be obtained from SAXS measurements where additionally the lamella thickness and long period can be measured assuming a model of lamella staples with alternating changes in the electron density.<sup>31,32</sup> In most cases it is assumed that the crystalline regions have a high electron density whereas the amorphous regions have a low electron density (an exception is for example syndiotactic poly-

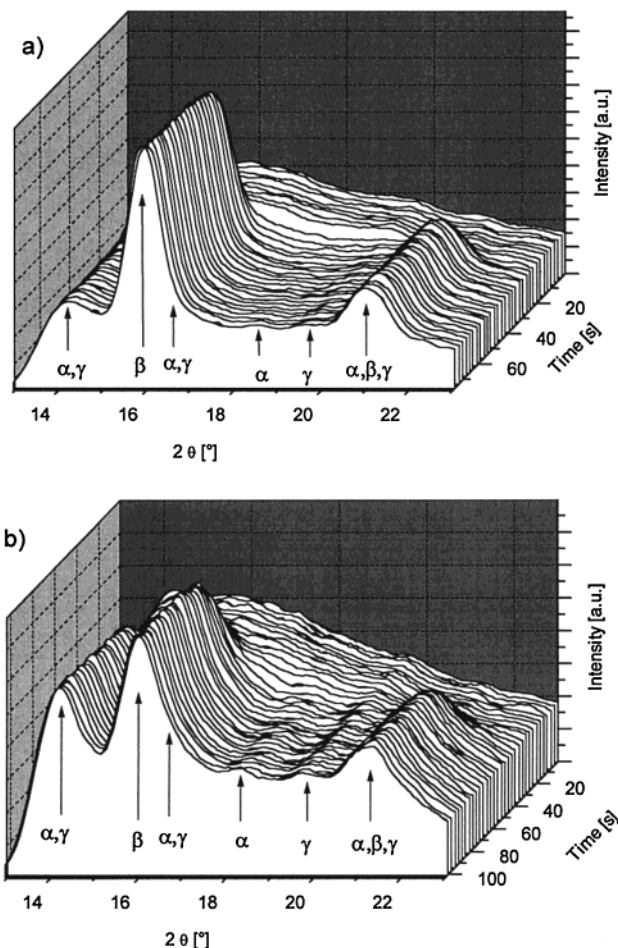


**Figure 3.** Time-resolved WAXS traces obtained after a temperature jump from  $190^\circ\text{C}$  to the crystallization temperature: (a) i-PP with 0.3 wt %  $\beta$ -NA at  $115^\circ\text{C}$ ; (b) i-PP-co-E-2.8 with 0.3 wt %  $\beta$ -NA at  $120^\circ\text{C}$ .

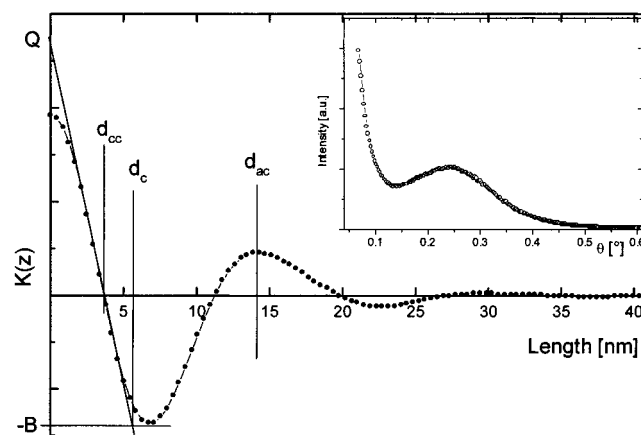


**Figure 4.** Correlation function  $K(z)$  of neat i-PP isothermally crystallized at  $115^\circ\text{C}$ . For explanation of data evaluation see text. The inset depicts the original SAXS trace.

styrene). The ideal model can be varied by assuming an extended interface between crystalline and amorphous regions or even by proposing a three-phase model.<sup>35</sup> Our data evaluation is based on a two-phase model assuming amorphous regions and crystalline regions with uniform electron density. Figure 4 shows the one-dimensional correlation function  $K(z)$  and the schematic data evaluation derived for i-PP after isothermal crystallization at  $T_c = 115^\circ\text{C}$ . The inset shows the original SAXS data. The first maximum of the



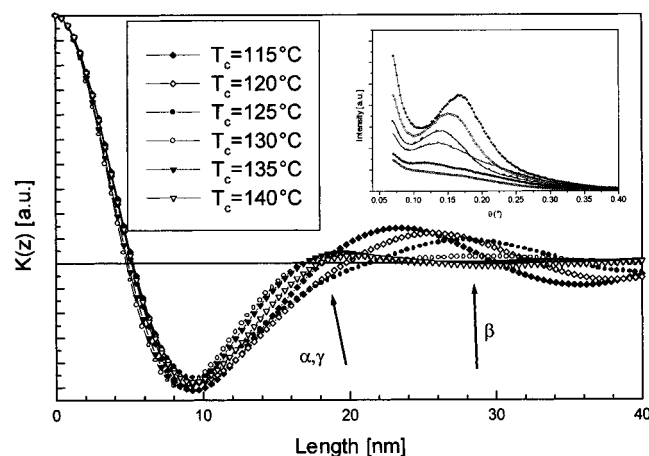


**Figure 5.** Normalized correlation function for i-PP with 0.3 wt %  $\beta$ -NA obtained at different crystallization temperatures after complete crystallization. The inset shows the original SAXS traces.

correlation function, i.e., the long period  $d_{ac}$ , corresponds to the length of the repeating units of crystalline and amorphous layers in the crystalline stacks.<sup>36</sup> The thickness of the smaller layer (either the crystalline or the amorphous) is represented by the length  $d_c$ . The “self-correlating triangle” at the origin is framed by the baseline, which limits the curve at the first minimum ( $-B$ ), and a straight line as linearized shape of the curve at the beginning. The intensities  $Q$  and  $B$  can be used to calculate the electron density difference  $\Delta\rho$  between the amorphous and the crystalline phase. The crystallinity as volume fraction of the crystalline parts in the lamellae stacks can be calculated via  $\phi = Q/(B + Q) = d_{cc}/d_c$ , but there remains an uncertainty whether  $\phi$  or  $1 - \phi$  is the correct value for the crystallinity. In the case that  $\phi$  is not very close to 0.5 the decision can be made employing WAXS data. An additional confirmation for  $\phi$  is the equation  $d_{cc} = \phi(1 - \phi)d_{ac}$ , which is independent of the determination of  $B$ .

The samples without  $\beta$ -NA do not show any  $\beta$ -modification, and from the SAXS traces the long period and the overall crystallinity are well detectable. Samples with 0.3 wt %  $\beta$ -NA have significant peaks in the WAXS traces for the  $\beta$ -modification as discussed above. The peak intensities of the  $\alpha$ - and  $\gamma$ -modification in the samples without ethene but with  $\beta$ -NA show a clear temperature dependence. With increasing crystallization temperatures above 125 °C, the amount of the  $\alpha$ - and  $\gamma$ -modification increases in addition to the dominating  $\beta$ -modification. This behavior can also be detected by SAXS measurements as shown in Figure 5. The normalized correlation functions of i-PP with 0.3 wt %  $\beta$ -NA isothermally crystallized at different temperatures derived from the corresponding SAXS traces shown in the inset of Figure 5 are depicted. The measured decreasing intensity for higher crystallization temperatures is due to a decrease in crystallinity and sample thickness. From the correlation function a significant long period can be detected for the crystallization temperatures 115 and 125 °C. The long period increases from 23 to 28 nm. At a crystallization temperature of 125 °C a small shoulder in the correlation function at 17 nm can be identified (marked by an arrow  $\alpha, \gamma$ ). At elevated crystallization temperatures (between 130 and 140 °C) the curve between 16 and 40 nm becomes very flat. It consists of two small local maxima: one at a shorter length close to the shoulder at about 18 nm and

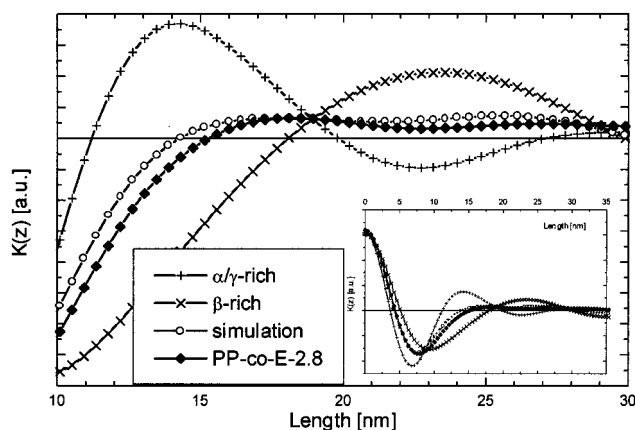


**Figure 6.**  $K(z)$  measured for PP-co-E-2.8 with 0.3 wt %  $\beta$ -NA after isothermal crystallization at 115 °C. Simulation of a correlation function  $K(z)$  assuming additivity for a sample containing nearly exclusively the  $\alpha/\gamma$ -modification (i-PP,  $T_c = 115$  °C) and nearly exclusively the  $\beta$ -modification (i-PP + 0.3 wt %  $\beta$ -NA,  $T_c = 115$  °C).

the other one at 30 nm and above (very weak, marked by an arrow  $\beta$ ).

The origin of the occurrence of two different long periods for crystallized i-PP is given by the different equilibrium melting points of the  $\alpha$ -,  $\beta$ -, and  $\gamma$ -modifications. The shoulder and the arising peak at about 18 nm are the result of a partial crystallization of i-PP in its  $\alpha$ - or  $\gamma$ -modification whereas at lower crystallization temperatures the  $\beta$ -modification is by far predominant. These results are identical with that obtained from WAXS measurements discussed above. The crystallite thickness depends inversely on the supercooling according to the Gibbs–Thomson equation. The  $\beta$ -modification with an equilibrium melting point in the range of 174 °C forms thicker crystallites at an identical crystallization temperature than the  $\alpha$ - or  $\gamma$ -modification with equilibrium melting points given in the literature between 188 and more than 200 °C.<sup>37</sup> Furthermore, it has been known that the typical crosshatching of the  $\alpha$ -modification, a kind of homoepitaxial growth, does not appear in the  $\beta$ -modification.<sup>38</sup> This may have a substantial contribution on the melting behavior due to the fact that the crystal thickness of the crosshatched lamellae is thinner compared to that of the mother lamellae. This may lead to the appearance of two melting points of i-PP in the  $\alpha$ -modification after isothermal crystallization at one supercooling temperature.

The random copolymers PP-co-E-2.8 and PP-co-E-5.7 with  $\beta$ -NA show in all measurements large amounts of the  $\beta$ - and  $\gamma$ -modification, even at crystallization temperatures between 115 and 125 °C. This distinguishes them from the i-PP sample with  $\beta$ -NA, which crystallizes in this temperature range nearly completely in the  $\beta$ -modification. In Figure 6 the correlation function in the area between 10 and 30 nm for PP-co-E-2.8 with  $\beta$ -NA isothermally crystallized at 115 °C is shown. In Figure 1b the corresponding WAXS measurement is represented by full circles.

The complete correlation functions are depicted in the inset. A single long period cannot be detected; the area is flat and extended. The shape of the curve can be simulated by a simple combination of the measured correlation function of an  $\alpha$ - and  $\gamma$ -rich sample (i-PP crystallized at 115 °C, see Figure 4) and a  $\beta$ -rich sample (i-PP with  $\beta$ -NA crystallized at 115 °C), as indicated in

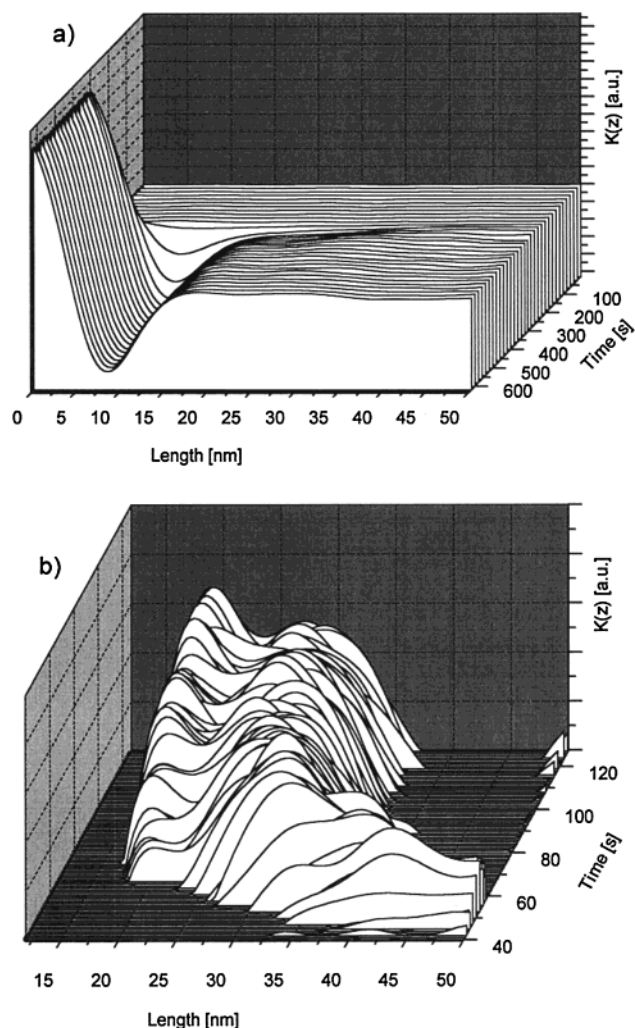


**Figure 7.** (a) Time-resolved correlation function  $K(z)$  for i-PP-co-E-2.8 with 0.3 wt %  $\beta$ -NA obtained at a crystallization temperature of 115 °C. (b) Enlarged area of  $K(z)$  in the range of the first maximum.

Figure 6. Although the samples differ in their ethene content, the simulated curve derived from an addition of the single correlation functions fits the experimental findings quite well. The different long periods can be distinguished from each other while the thickness of the crystalline or amorphous layer from the first minimum of the correlation function yields only a single mean value. The measured value is determined by the thickness distribution of crystallites, which is not sharp; otherwise, a plateau in the correlation function arises in the range of the first minimum.

In Figure 7a the time-resolved correlation function  $K(z)$  for i-PP-co-E-2.8 with 0.3 wt %  $\beta$ -NA obtained at a crystallization temperature of 115 °C after a quenching step from 190 °C is depicted. To identify the temperature dependence of the long period, an enlarged area of the correlation function  $K(z)$  in the range of the first maximum is shown in Figure 7b. In the beginning of the crystallization a peak at about 42 nm can be identified. With increasing crystallization time this long period decreases to 30 nm, and after about 350 s a second peak at 20 nm appears. As stated above, the larger long period belongs to the  $\beta$ -modification which therefore dominates the crystallization at early times. The smaller long period is associated with the occurrence of  $\alpha$ - and  $\gamma$ -crystallites. The samples with pre-

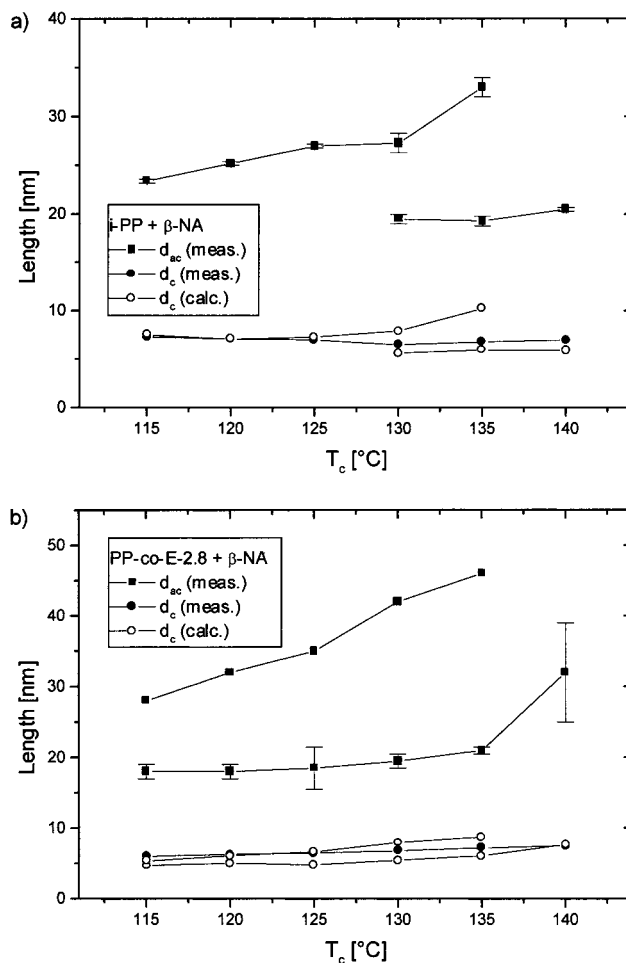


**Figure 8.** Long period and lamella thickness from SAXS measurements for (a) i-PP with 0.3 wt %  $\beta$ -NA and (b) PP-co-E-2.8 with 0.3 wt %  $\beta$ -NA. The full symbols correspond to measured values while the open circles are calculated from long period and crystallinity.

dominantly  $\alpha$ -modification (i-PP) have the highest crystallinity of about 35% at the lower crystallization temperatures and 30% at the higher ones, and they show the shortest long periods between 13 and 16 nm. With increasing  $\gamma$ -content (random copolymers) the crystallinity is 3% less, and the long period increases in the same manner. The crystallinity of samples including a large amount of  $\beta$ -modification (nucleated samples) decreased for another 3%, and the long periods are shifted to a length between 23 and 30 nm.

In Figure 8 the results from SAXS measurements for  $\beta$ -nucleated i-PP (Figure 8a) and PP-co-E-2.8 (Figure 8b), isothermally crystallized at different temperatures between 115 and 140 °C, are depicted. The long period, i.e., the length  $d_{ac}$ , splits into two paths if besides the  $\beta$ -modification a significant amount of  $\alpha$ - and  $\gamma$ -modification is formed. The long period with the larger length scale is in continuation to the long period determined at lower temperatures and is therefore associated with the  $\beta$ -modification. The long period arising at shorter lengths as written above is related to the  $\alpha$ - and  $\gamma$ -modification. For the lamella thickness only a single value is measured even in the case that two different types of lamellae are present. The crystalline lamella thickness calculated from long period and crystallinity (determined from the  $d_{ac}$  and  $d_{cc}$ <sup>36</sup>) is depicted by open circles. For samples with one dominating modification this length is nearly the same when measuring the

lamella thickness  $d_c$  from the correlation function directly. When two or more modifications arise with different long periods (and lamellae thickness), the direct analysis gives an average value of the indirectly calculated length. The  $\beta$ -modification has, caused by the lower equilibrium melting point, enlarged lamellae.

## Conclusions

Simultaneous WAXS and SAXS measurements are capable of determining the time- and temperature-resolved formation of the  $\alpha$ -,  $\beta$ -, and  $\gamma$ -modification of isotactic polypropylene and random copolymers of propene and ethene. By using a metallocene i-PP, the formation of the  $\gamma$ -modification increases compared to the  $\alpha$ -modification, which is nearly exclusively formed during the crystallization of conventional high molar mass Ziegler–Natta type polypropylene. This effect is even enhanced by adding a small amount of ethene or other 1-olefins to the polymer. But the two types of polymers, metallocene i-PP (with relatively large amounts of stereo- and regioirregularities, 1.1% defects) and the random copolymers where the monomer units of ethene can be considered as defects in the polymer helix, behave differently when a  $\beta$ -NA is added prior to crystallization. The i-PP samples are able to crystallize nearly exclusively in  $\beta$ -modification when isothermally crystallized between 115 and 125 °C, while the random copolymers always crystallize to a large extent in the  $\alpha$ - and  $\gamma$ -modification for all crystallization temperatures under investigation. From the temperature dependence of the different amounts of  $\alpha$ -,  $\beta$ -, and  $\gamma$ -modification the long periods, derived from SAXS measurements, can be assigned. The long period of the  $\beta$ -modification is much larger than the other ones, so smaller long periods within the lamella stacks can be detected simultaneously.

**Acknowledgment.** We thank the Fonds der Chemischen Industrie for financial support.

## References and Notes

- Brückner, S.; Meille, S. V. *Nature* **1989**, *340*, 455.
- Kardos, J. L.; Christiansen, E.; Baer, E. *J. Polym. Sci. A-2* **1966**, *4*, 777.
- Pae, K. D.; Morrow, D. R.; Sauer, J. A. *Nature* **1966**, *211*, 514.
- Turner-Jones, A. *Polymer* **1971**, *12*, 487.
- Guidetti, G. P.; Busi, P.; Giulianetti, I.; Zanetti, R. *Eur. Polym. J.* **1983**, *19*, 757.
- Busico, V.; Corradini, P.; De Rosa, C.; Di Benedetto, E. *Eur. Polym. J.* **1985**, *21*, 239.
- Avella, M.; Martuscelli, E.; Della Volpe, G.; Segre, A.; Rossi, E.; Simonazzi, T. *Makromol. Chem.* **1986**, *187*, 1927.
- Arnold, M.; Bornemann, S.; Köller, F.; Menke, T. J.; Kressler, J. *Macromol. Chem. Phys.* **1998**, *199*, 2647.
- Marigo, A.; Marega, C.; Zanetti, R.; Paganetto, E.; Canossa, E.; Coleta, F.; Gottardi, F. *Makromol. Chem.* **1989**, *190*, 2805.
- Mezghani, K.; Phillips, P. J. *Polymer* **1995**, *35*, 2407.
- Fischer, D.; Mülhaupt, R. *Makromol. Chem. Phys.* **1994**, *195*, 1143.
- Jüngling, S. PhD Thesis, Freiburg, 1995.
- Kressler, J. In *Polypropylene: An A–Z Reference*; Karger-Kocsis, Ed.; Kluwer Acad. Publ.: Dordrecht, 1999; p 267.
- Padden, H. J.; Keith, H. D. *J. Appl. Phys.* **1959**, *30*, 1479.
- Keith, H. D.; Padden, F. J.; Walter, N. M.; Wyckoff, H. W. *J. Appl. Phys.* **1959**, *30*, 1458.
- Turner-Jones, A.; Aizlewood, J. M.; Beckett, D. R. *Macromol. Chem.* **1964**, *75*, 134.
- Varga, J.; Ehrenstein, G. W. In *Polypropylene: An A–Z Reference*; Karger-Kocsis, Ed.; Kluwer Acad. Publ.: Dordrecht, 1999; p 51.
- Mayer, R.-D.; Friedrich, C.; Mülhaupt, R. *Kunststoffe* **1999**, *89* (4), 89.
- Lotz, B.; Kopp, S.; Dorset, D. C. *R. Acad. Sci. Paris IIb* **1994**, *319*, 187.
- Lotz, B.; Wittmann, J. C.; Lovinger, A. J. *Polymer* **1996**, *37*, 4979.
- Ferro, D. R.; Brückner, S.; Meille, S. V.; Ragizzi, M. *Macromolecules* **1992**, *25*, 5231.
- Meille, S. V.; Ferro, D. R.; Brückner, S. *Polym. Prepr. (Am. Chem. Soc., Div. Polym. Chem.)* **1992**, *33* (1), 268.
- Ferro, D. R.; Meille, S. V.; Brückner, S. *Macromolecules* **1998**, *31*, 6926.
- An, B. *Acta Polym. Sin.* **1993**, *3*, 330.
- Meille, S. V.; Brückner, S.; Porzio, W. *Macromolecules* **1990**, *23*, 4114.
- Lotz, B.; Wittmann, J. C.; Lovinger, A. J. *Polymer* **1996**, *37*, 4979.
- Thomann, R.; Wang, C.; Kressler, J.; Mülhaupt, R. *Macromolecules* **1996**, *29*, 8425.
- Galeski, A. In *Polypropylene: An A–Z Reference*; Karger-Kocsis, Ed.; Kluwer Acad. Publ.: Dordrecht, 1999; p 135.
- Natta, G.; Corradini, P.; Cesari, M. *R. C. Accad. Lincei* **1956**, *21*, 365.
- Wutz, C. Ph.D. Thesis, Shaker, Aachen, 1993.
- Strobl, G. R.; Schneider, M. J.; Voigt-Martin, I. G. *J. Polym. Sci.* **1980**, *18*, 1361.
- Tanabe, Y.; Strobl, G. R.; Fischer, E. W. *Polymer* **1986**, *27*, 1147.
- Lotz, B.; Fillon, B.; Thierry, A.; Wittmann, J. C. *Polym. Bull.* **1991**, *25*, 101.
- Li, J. X.; Cheung, W. L.; Jia, D. *Polymer* **1999**, *40*, 1219.
- Feigin, L. A.; Svergun, D. I. *Structure Analysis by Small-Angle X-Ray and Neutron Scattering*; Plenum Press: New York, 1987.
- Strobl, G. *The Physics of Polymers*; Springer: Berlin, 1997.
- Phillips, P. J.; Mezghani, K. In *The Polymer Materials Encyclopedia*; Salamone, J. C., Ed.; CRC Press: Boca Raton, FL, 1996; Vol. 9, p 6637.
- Moore, E. P. Jr., Ed. *Polypropylene Handbook*; Hansa Publishers: Munich, 1996.

MA000719R